JOURNAL OF AIRCRAFT
Vol. 38, No. 3, May–June 2001

Oscillatory Control of Shock-Induced Separation

Avi Seifert* and LaTunia G. Pack†
NASA Langley Research Center, Hampton, Virginia 23681-2199

An experimental investigation, aimed at delaying flow separation as a result of the occurrence of a shock-wave/boundary-layer interaction, is reported. The experiment was performed using a NACA 0015 airfoil at high-Reynolds-number incompressible and compressible flow conditions. The effects of Mach and Reynolds numbers were identified, using the capabilities of the cryogenic-pressurized facility to maintain one parameter fixed and change the other. The main objectives of the experiment were to study the effects of periodic excitation on airfoil drag divergence and to alleviate the severe unsteadiness associated with shock-induced separation (known as *buffeting*). Zero-mass-flux oscillatory blowing was introduced through a downstream directed slot located at 10% chord on the upper surface of the NACA 0015 airfoil. The effective frequencies generated 2–4 vortices over the separated region, regardless of the Mach number. Even though the excitation was introduced upstream of the shock wave, it had pronounced effects downstream of it. Wake deficit (associated with drag) and unsteadiness (associated with buffeting) were reduced. The spectral content of the wake pressure fluctuations indicates steadier flow throughout the frequency range when excitation is applied. This is especially evident at low frequencies which are more likely to interact with the airframe.

Nomenclature

a	=	speed of sound, $\equiv \sqrt{(\gamma RT)}$
C_d	=	total drag coefficient
C_{dp}	=	form drag coefficient
C_l	=	lift coefficient
C_p	=	pressure coefficient, $\equiv (P - P_s)/q$
C'_p	=	fluctuating pressure coefficient, $\equiv p'/q$
c	=	airfoil chord
$\langle c_\mu \rangle$	=	oscillatory blowing momentum coefficient, $\equiv h/c(1 + T_\infty/T_j)(\langle u' \rangle/U_\infty)^2$
F^+	=	reduced frequency, $\equiv f x_{te}/U_\infty$
f	=	frequency, Hz
h	=	slot height or width
M	=	Mach number, $\equiv U_\infty/a$
P	=	pressure
q	=	freestream dynamic pressure, $\equiv \frac{1}{2}\rho U_\infty^2$
R_c	=	chord Reynolds number, $\equiv U_\infty c/\nu$
T	=	temperature
U, u	=	averaged and fluctuating velocity
X/c	=	normalized streamwise location
x_{te}	=	distance from actuator to airfoil trailing edge
Y/c	=	distance normal to airfoil surface
Z	=	spanwise location
α	=	airfoil angle of attack, deg
Δ	=	difference between baseline and controlled parameter
ν	=	kinematic viscosity
ρ	=	density
$\langle\ \rangle$	=	phase-locked values

Subscripts

j	=	conditions at blowing slot
max	=	conditions at maximum lift
s	=	tunnel static conditions
∞	=	freestream conditions

Superscripts

crit	=	critical Mach number
res	=	acoustic resonance frequency
‘	=	rms of fluctuating value

Presented as Paper 99-0925 at the 37th Aerospace Sciences Meeting, Reno, NV, 11–14 January 1999; received 23 March 1999; revision received 21 October 1999; accepted for publication 8 September 2000.

*Currently Senior Lecturer, Department of Fluid Mechanics and Heat Transfer, Faculty of Engineering, Tel-Aviv University, Ramat-Aviv 69978, Israel. Senior Member AIAA.

†Research Engineer, Flow Physics and Control Branch.

I. Introduction

FLOW separation at compressible speeds typically occurs downstream of a shock-wave/boundary-layer interaction. The pressure jump across the shock either causes immediate separation or thickens the boundary layer and reduces its momentum such that it separates further downstream. Once the flow separates downstream of the shock, the unsteady separation and subsequent reattachment (if it occurs) induce unsteadiness both in the shock position and strength. This phenomenon is known as *buffeting*. The low-frequency oscillations can cause structural damage, if coupled with the resonance frequencies of the structure. When the operation envelope includes transonic speeds, the strength of the shock can be minimized using proper shaping (e.g., supercritical airfoils). However, at off-design or transient flight conditions, detrimental or even dangerous effects can take place. Various passive control methods were developed to alleviate these effects. Porous strips and wall bumps[1] are effective in reducing the strength of the shock wave. Vortex generators (mechanical[2] or canted jets[3]), as well as suction through slots, are effective at controlling shock-induced separation. The feedback loop causing buffet is effectively eliminated by proper placement of porous strips and underside cavities.

Vortex generators were numerically simulated to control shock-wave/boundary-layer interaction and alleviate buffet.[4] This was achieved by energizing the boundary layer upstream of the shock wave by pairs of counter-rotating vortices. Although placed upstream, the main effect was a smaller separation bubble downstream of the shock. As a result of the thinner boundary layer, the shock strength increased, as did the rate of pressure recovery downstream of it. The calculated pressures are in qualitative agreement with experiment.[2]

The effects of suction through slots and a porous surface, on the performance of a supercritical airfoil at off-design conditions, were tested experimentally.[5] The double slot and perforated plate were very effective in reducing drag and less effective at increasing poststall lift, even without the suction. This was possible because the cavity underneath allowed mass transfer from the downstream side of the shock (high pressure) to the upstream side of it. In the steady sense the suction downstream of the shock reduced the boundary-layer tendency to separate, whereas the upstream bleed from the

surface thickened the boundary layer and reduced the shock strength. This in turn reduced the tendency for separation downstream. The double slot was especially effective in buffet alleviation, completely eliminating the shock-wave/separated flow coupling. The physical mechanism producing this effect was not identified.

To be efficient, the methods just mentioned need to be actively controlled. Bump position, height, and shape need to be tailored to each specific flow condition. Porous strips, which need to cover about 10% of the chord, cause transition on laminar airfoils and increase skin-friction drag. Porosity and slot locations also need to be mission tailored. Although these devices could be designed to widen the flight envelope to a certain extent, their application for guidance and control, which requires fast response,[6] is doubtful. Furthermore, efficiency considerations rule out the use of tangential blowing, and stealth considerations rule out the use of mechanical vortex generators. Therefore, fast responding, active methods for management of high lift as well as compressible unsteady flows are studied.

Low-Reynolds and Mach-number studies (Ref. 7–9 and references therein) have shown that periodic vortical excitation introduced into a separating boundary layer, slightly upstream of the average separation location, can effectively delay boundary-layer separation. The improved ability of the boundary layer to overcome an adverse pressure gradient is attributed to enhanced mixing between the low-momentum fluid near the wall and the external high-momentum flow. The successful application of the method increases the lift while maintaining low drag. At low Mach numbers, where high lift for takeoff, landing, or loiter is required, the delay of boundary-layer separation allows increased loading of a multielement high-lift airfoil system.

It was recently demonstrated[10] that periodic excitation can delay boundary-layer separation from airfoils at flight Reynolds numbers and incompressible speeds. Low-Reynolds-number experiments, where control was applied from the leading-edge (LE) region of the airfoils, were repeated at a chord Reynolds number of 37.6×10^6. Using a flapped NACA 0015 airfoil, where control was applied at the flap shoulder, it was shown that the method is essentially independent of Reynolds number.[10] A recently published numerical simulation[11] shows that oscillatory excitation of a separated boundary layer, at low Reynolds and Mach numbers, can significantly increase poststall lift at excitation frequencies that are 0.3–4 times the natural vortex shedding frequency ($F^+ = 0.4$ in this case). By using frequencies that are at least twice the shedding frequency, which correspond to our definition of $F^+ \approx 0.8$, the lift enhancement is accompanied by a significant reduction in drag and drag excursions (Figs. 6 and 7 in Ref. 11). Indications of these effects were experimentally identified in Ref. 10. Using an appropriate combination of frequency ($F^+ \approx 1$) and magnitude ($\langle c_\mu \rangle = 10$ to 50×10^{-5}), the flow should be steadier, even if it is intermittently separated. Similar trends, at least for the lift increment and the excitation F^+, were also identified numerically.[12]

The present knowledge on active control of flow separation at compressible speeds is very limited. One encouraging result is reported in Ref. 13, which shows that by rotating a flat plate downstream of an airfoil experiencing shock-induced separation the extent of separated flow could be affected. The reduced forcing frequency was close to the airfoil buffeting frequency, $F^+ \approx 0.1$. These frequencies are too low for effective separation control.

The nature of the device used to control the shock-induced separation is not important, as long as the resulting vortical excitation is at sufficient amplitude and appropriate frequency. Two-dimensional, wall-tangential oscillatory blowing[7,10] is currently used because the magnitude, the frequency, and the average mass flux are conveniently controllable, whereas the airfoil geometry is almost unchanged as a result of the narrow blowing slots.

The objectives of the present investigation are the following: 1) to enhance performance and reduce flow unsteadiness in incompressible speeds and to determine the relationship between the controlled excitation and the naturally occurring unsteady flow in the presence of separated flows, and 2) to suppress shock-induced separation and provide buffet alleviation by using periodic excitation.

II. Experimental Setup

A. Overview

The experiment was conducted in the 0.3-m Transonic Cryogenic Tunnel at NASA Langley Research Center, using gaseous nitrogen (GN_2) as the test fluid. The execution of an active flow control experiment in a pressurized cryogenic wind tunnel has advantages and disadvantages. For example, a cryogenic pressurized facility allows independent control of R_c and M at a fixed freestream velocity. With this type of control, the effective frequencies are clearly indicated because F^+ can be held fixed when R_c is varied and M is held constant or R_c is fixed while M is varied. Another advantage of testing in a cryogenic pressurized facility is the ability to generate a zero-mass-flux disturbance when using an oscillatory blowing valve. One of the disadvantages of testing in a cryogenic pressurized facility is that an in situ determination of $\langle c_\mu \rangle$ is very difficult. However, using atmospheric bench-top tests and a simplified flow model it is possible to estimate the $\langle c_\mu \rangle$ used.[10]

A new diagnostic tool was used in this experiment. It consists of a wake rake that was instrumented with dynamic pressure transducers. Its calibration and the methodology of data processing are presented in the following sections. A conventional NACA 0012 airfoil was tested in order to validate the new rake and to acquire unsteady wake data over a smaller chord, smooth airfoil.[14] The straight NACA 0015 airfoil was tested with control applied from the LE region.

The experiments were conducted at Mach numbers of 0.2–0.65 and chord Reynolds numbers ranging from 1.5×10^6 to 23.5×10^6.

B. Wind Tunnel

The experiment was conducted in the 0.3-m Transonic Cryogenic Wind Tunnel at the NASA Langley Research Center. It is a closed-loop, fan-driven tunnel with a test cross section of 0.33×0.33 m. GN_2 was the test medium. The tunnel operates at stagnation pressures ranging from 1.2 up to 6 bar and total temperatures from 78 up to 327 K.[15,16] The floor and ceiling of the tunnel were diverged by 0.3–0.4 deg in the vicinity of the airfoil to reduce blockage resulting from boundary-layer growth on the test-section walls. A wake survey rod extends from the left tunnel sidewall to vertically traverse the airfoil wake (see Fig. 1). Details about the wake data acquisition system are provided in Sec. II.F.

Wall pressures were acquired together with the airfoil pressures at all test conditions. This information could be used later for numerical simulation of the flow taking into consideration wall interference effects.

C. Airfoil

The experiments were conducted on a NACA 0015 airfoil ($c = 254$ mm, Fig. 2), equipped with a blowing slot at 10% chord, suitable for the control of separation near the LE. The slot was about 0.2% chord wide (0.5 mm) and allowed an almost tangential

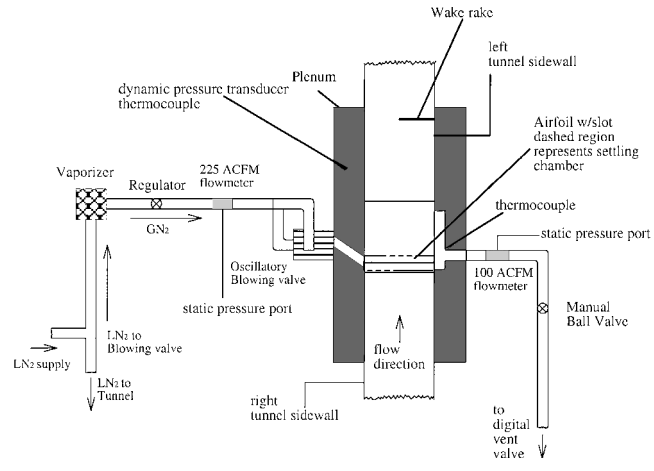

Fig. 1 Schematic description of the experimental setup in the 0.3-m Transonic Cryogenic Wind Tunnel (top view).

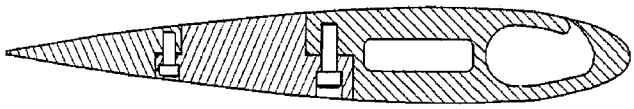

Fig. 2 NACA 0015 airfoil with a blowing slot at $X/c = 10\%$.

streamwise introduction of the excitation. The tunnel pressure scanning system recorded the airfoil 50 static-pressure taps and test-section wall pressures.

D. Oscillatory Blowing System

A rotating, siren-type, valve was used to generate the pressure oscillations inside the airfoil cavity.[10] The oscillatory blowing valve was upgraded and is presently capable of generating frequencies up to 800 Hz and fluctuating pressure levels of 5 psi. For safety reasons the valve was rated to 300 psi. GN_2 was supplied to the valve by converting a portion of the liquid nitrogen available for operating the tunnel using an ambient temperature vaporizer. The use of ambient temperature GN_2 simplified the valve design. A pressure regulator controlled the GN_2 entering the valve and the variable speed drive of the valve motor controlled the frequency of the pressure oscillations. The oscillatory blowing valve was attached to the right tunnel plenum door at the center of rotation of the turntable (Fig. 1). A 49-mm i.d. pipe connected the valve to the LE cavity. The exhaust side of the airfoil cavity was connected to the tunnel boundary-layer removal system. The valves in the boundary-layer removal system controlled the flow rate out the exhaust side of the airfoil cavity (Fig. 1). Any relevant combination of steady and oscillatory blowing could be generated with this type of control. However, all of the results presented in this paper are for zero-mass-flux excitation.

E. Bench-Top Experiments

The phase-locked pressure fluctuations ($\langle p' \rangle$) at the entrance to the airfoil cavity were measured both in situ and with bench-top tests. The correlation between $\langle u'^2 \rangle$ and $\langle p' \rangle / \rho$ (derived from the bench-top tests) is used to calculate the $\langle c_\mu \rangle$ in the cryogenic tests.[10]

The velocity fluctuations exiting the slots of the airfoil were measured with the airfoil outside the tunnel using a hot-wire mounted on a three-dimensional traverse system. The GN_2 supplied to the oscillatory blowing valve during the wind-tunnel test was replaced with compressed air. All of the pipe accessories were identical in both the wind-tunnel and the bench-top experiments in order to maintain similarity between the two experiments. Although any desired combination of oscillatory and steady flow rates were obtainable in the wind-tunnel experiment, steady suction could not be applied in the bench-top experiments because of the atmospheric test conditions. However, even in the bench-top experiments, reverse flow in the slot was encountered as a result of the instantaneous, subatmospheric pressures created by the inertia of the continuous flow along the airfoil cavity. The signals from the dynamic pressure transducer and the hot wire were acquired using a 16-bit high-speed A/D converter, coupled with an antialiasing filter. In the cases where reverse flow was expected at the slot exit, the hot-wire signal was derectified to account for the reverse flow.[10]

F. Dynamic Wake Rake

The wake of the airfoils was traversed using the tunnel standard wake survey rake and a modified wake rake, instrumented with two dynamic pressure transducers and seven total pressure tubes. The modified wake rake enables the recording of unsteady wake data, phase locked to the controlled excitation. The dynamic wake rake was located two chords downstream of the NACA 0015 airfoil midchord.

Figure 3 presents a picture of the dynamic wake rake. The dynamic pressure transducers were installed inside tubes 2 and 4 of the rake. The tubes were displaced 12.7 mm in the spanwise direction, while tube #1 was located 38.1 mm from the tunnel centerline. Because of the relatively large outer diameter of the transducer (2.36 mm), which could adversely affect the measurement of the

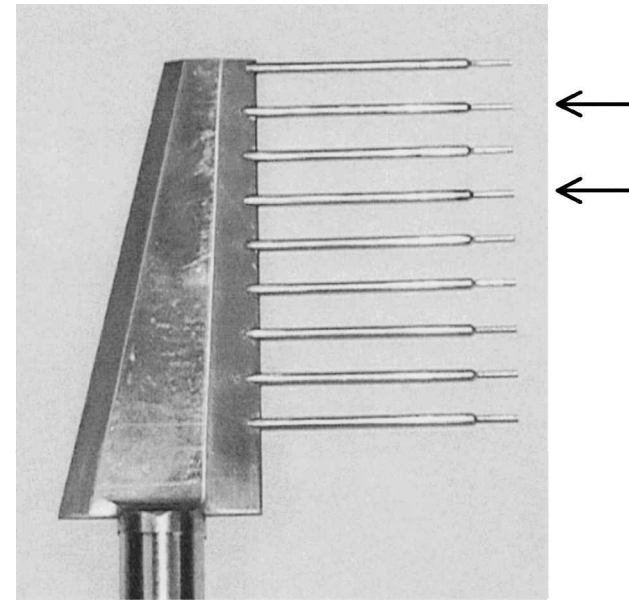

Fig. 3 Wake rake with dynamic pressure transducers (← indicate instrumented tubes), tube spacing: 12.7 mm.

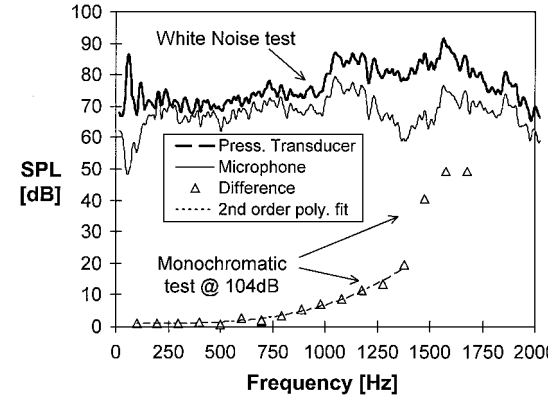

Fig. 4 Frequency response of the dynamic wake rake.

wake dynamic pressure, the decision was made to use a smaller diameter tube (1.60 mm O.D. and 1.03 mm I.D.), about 30 mm long, from the transducer's face to the measuring location. The length and internal volume of this tube can change the frequency response of the tube-transducer system as a result of acoustic resonance. A calibration was performed by placing a sound source in front of the wake rake, inside the wind-tunnel test section at atmospheric conditions, without flow in the tunnel. The sound was either white noise or discrete tones. A microphone was positioned next to the tubes. The signals from the two dynamic pressure transducers were recorded along with the microphone output. These results are used to correct the signals measured under various tunnel conditions, assuming that the only variant is the flow temperature (which affects the speed of sound).

Figure 4 presents the results of the white noise and discrete tone testing. The white-noise results show that the microphone and the dynamic pressure transducer measure similar noise levels (± 2 dB) between 150 Hz and 1 KHz. The discrete tone testing was performed at a resolution of about 100 Hz and at significantly higher sound pressure levels (SPL, about 104 dB) than the white-noise test. Figure 4 also presents the difference in the SPL between the dynamic pressure transducer and the microphone. Transducer #1 (position #2 in the wake rake, see Fig. 3) and the microphone measure similar SPL until 0.5 kHz. For frequencies above 0.6 kHz, the pressure transducer output increases monotonically with respect to the microphone output. The difference peaks at about 1.5 kHz where the pressure transducer output is about 50 dB higher than the microphone output. Examining

Table 1 Experimental uncertainties

Item	Uncertainty, % F.S.	Full scale and condition
Slot width	5	0.5 mm
Static temperature	0.3	300 K
Static pressure	1	70 psi, $M = 0.3$ and 100 K
R_c	2.0	$M < 0.3$
R_c	1.0	$M > 0.3$
M	0.5	$M > 0.3$
F^+	1	2
$\langle c_\mu \rangle$	25	Local values

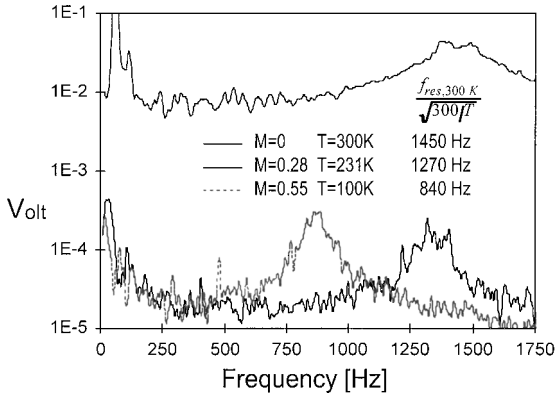

Fig. 5 Temperature effect on the resonance of the transducer-tube system of the dynamic wake rake.

again the results of the white-noise test and normalizing the pressure transducer output by the microphone output (the upper solid line in Fig. 5) reveals a flat response between 150 Hz and about 1 kHz. The transducer-tube system resonates at about 1.4–1.5 kHz, at ambient temperature. The SPL difference shown in Fig. 4 indicates that at $f/f_{\text{res}} = 0.95$ the difference is 20 dB, and a smooth line fits the data very well. The required pressure fluctuations attenuation factor was calculated using a second-order polynomial fit to the inverse of the SPL difference in the form

$$\text{Factor} = -1.076(f/f_{\text{res}})^2 + 0.1343(f/f_{\text{res}}) + 0.905 \qquad (1)$$

The acoustic resonance frequency is temperature dependent and was found to scale, as expected, inversely with the square root of the temperature ratio. This point is illustrated by the additional data shown in Fig. 5. The $M = 0.28$ and 0.55 data were acquired outside the airfoil wake. The resonance frequencies correlate very well with the expected changes in the resonance frequency, based on the temperature of the tunnel flow.

G. Experimental Uncertainty

The incompressible experiments are conducted at conditions close to the limits of the wind-tunnel operating envelope. For example, the very low temperatures (about 100 K) and Mach numbers (0.28) are close to the limits of the tunnel capability. Most of the baseline data were acquired with separated regions or shock waves present on the airfoil. Tunnel wall interference will be considered at a later stage, as the tunnel wall pressures were recorded along with the airfoil and wake data. The movable walls of the test section were slightly diverged to reduce the effects of boundary-layer growth. Tables 1 and 2 contain most of the relevant information regarding experimental uncertainties. These values were calculated using ±3 standard deviations of the various experimental conditions and calculated parameters (including repeated runs). All test instruments were calibrated prior to use.

The uncertainty regarding the calculated airfoil aerodynamic parameters is listed in Table 2 (in absolute values and related to flow condition).

Table 2 Accuracy of integral parameters

Parameter	Fully attached	Stalled	Controlled
C_l	0.01	0.03	0.015
C_{dp}	0.001	0.003	0.0015
C_d	0.001	0.003	0.002

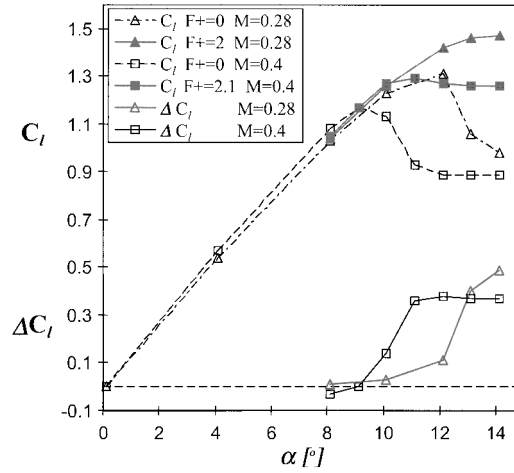

Fig. 6 Effects of Mach number and periodic excitation on the lift of the NACA 0015 airfoil. $R_c = 12.7 \times 10^6$, $\langle c_\mu \rangle = 0.03\%$ ($M = 0.28$), and 0.025% ($M = 0.4$).

III. Discussion of Results

A. Overview

The main challenges of active flow control at compressible speeds are drag reduction, delay of drag divergence, and suppression of unsteady aerodynamic loading along with its possible interaction with the structure (buffeting). The generation of high lift is less important than in low Mach numbers (takeoff, landing, and loiter flight).

There are a number of possible obstacles (for brevity we list here only three important obstacles) to the successful application of mixing enhancement using periodic excitation to transonic flows. First, it is not clear how the excitation evolves in the supersonic flow. It is known that compressibility reduces the amplification rate of shear-flow disturbances. Second, it is not thoroughly understood what effect shock waves have on vorticity fluctuations that are transported through them. Numerical and experimental evidence shows that turbulence,[17,18] shear waves,[19] and vortices[20,21] that pass through shock waves are being amplified and modify the shock in an unsteady manner. But most of these investigations were performed without the presence of a solid surface and a boundary layer. Third, it is not clear how downstream flow modification will affect the upstream supersonic flow. Because of the many unknown aspects of the problem, it was decided to start exploring active separation control in wholly incompressible flow ($M = 0.28$) and to gradually increase the Mach number while maintaining constant Reynolds number, wherever possible. These flow conditions provided shock-free flow ($M = 0.28$), a weak shock upstream of the excitation slot ($M = 0.4$), and a strong shock wave downstream of the slot ($M = 0.55$). Control was applied from the slot located at $X/c = 10\%$, and the excitation was of zero mass flux.

B. Separation Control over the Straight NACA 0015 Airfoil

Figure 6 presents the lift data of the NACA0015 airfoil at Mach numbers of 0.28 and 0.4 and at $R_c = 12.7 \times 10^6$. The baseline lift is presented by empty symbols and broken lines. Significant Mach-number effects can be seen even at the marginally compressible flow of $M = 0.4$. The baseline $C_l - \alpha$ slope increases by 7%, $C_{l,\max}$ drops from 1.31 to 1.17, and $\alpha_{\max}$ drops from 12 to 9 deg. When periodic excitation was applied to the airfoil at $M = 0.28$, with $F^+ = 2$ and $\langle c_\mu \rangle = 30 \times 10^{-5}$ stall is delayed from 12 to 14 deg,

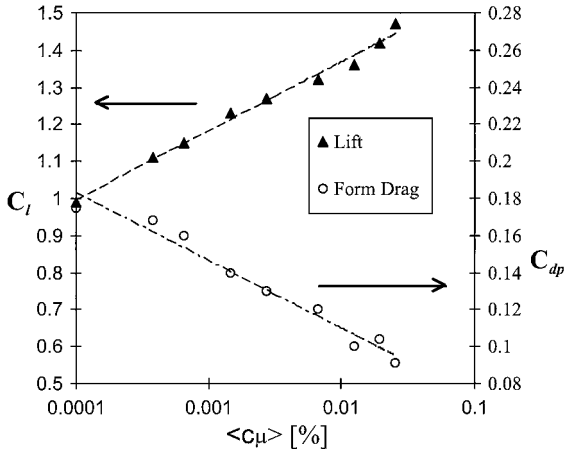

Fig. 7 Effects of excitation magnitude on the performance of the NACA 0015 airfoil. $\alpha = 14$ deg, $M = 0.28$, $R_c = 12.7 \times 10^6$.

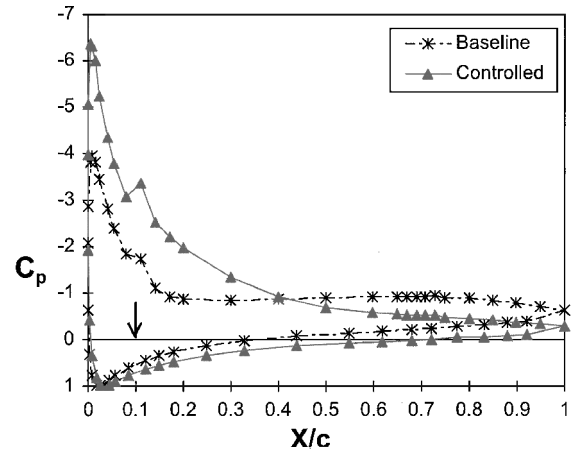

Fig. 8a NACA 0015 pressure coefficients. $M = 0.28$, $\alpha = 14$ deg, $R_c = 12.7 \times 10^6$, $F^+ = 2$, $\langle c_\mu \rangle = 0.03\%$. → indicates excitation slot.

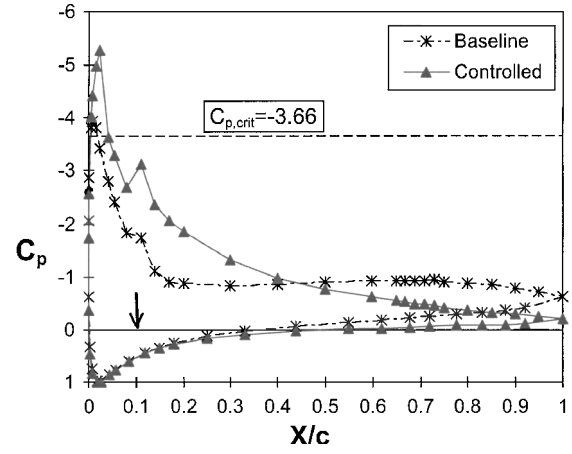

Fig. 8b NACA 0015 pressure coefficients. $M = 0.4$, $\alpha = 11$ deg, $R_c = 12.7 \times 10^6$, $F^+ = 2.1$, $\langle c_\mu \rangle = 0.025\%$. → indicates excitation slot.

and $C_{l,\max}$ increases from 1.31 to 1.47. When excitation was applied at $M = 0.4$, with $F^+ = 2.1$ and $\langle c_\mu \rangle = 25 \times 10^{-5}$ (Fig. 6) $\alpha_{\max}$ increases from 9 to 11 deg, and $C_{l,\max}$ increases from 1.17 to 1.29. The lift increment caused by the excitation is also plotted in Fig. 6. It shows that the significant lift increment, caused by the excitation, persists as M is increased from 0.28 to 0.4. One small difference could be observed at $\alpha = 8$ deg and $M = 0.4$, where the lift decreases slightly below the baseline as the excitation is activated.

The baseline form drag for $M = 0.4$ (not shown) is higher than that of the $M = 0.28$ data, as stall is approached. The small decrease in the controlled lift prior to stall at $M = 0.4$ (Fig. 6) is accompanied by a small increase in form drag. These detrimental effects were not observed at $M < 0.3$.

The effect of the excitation magnitude on the airfoil lift and form drag at $M = 0.28$ is presented in Fig. 7. Reproducing the effects found in the low R_c experiments,[8] as well as the controlled flap data at high R_c (Ref. 10), the lift increases, and the form drag decreases proportionally to the excitation $\langle c_\mu \rangle$. Saturation has not been reached at the available momentum coefficients. As indicated by the straight lines, the trends are almost logarithmic. The increased $C_l - \langle c_\mu \rangle$ slope for $\langle c_\mu \rangle > 10 \times 10^{-5}$ is probably a result of increased interference with the tunnel walls (wall corrections were not applied). The decrease rate of the form drag is initially slower than the increase rate of the lift.

Figure 8a presents the baseline and controlled airfoil surface-pressure distributions at $\alpha = 14$ deg and $M = 0.28$. The baseline C_p indicates that the flow separates at $X/c = 0.15$. When excitation is applied from the slot located at $X/c = 0.1$, the suction peak becomes significantly stronger, and an effective pressure recovery is restored, downstream of the slot. $C_{p,\mathrm{TE}}$ becomes more positive, indicating the increased tendency of the flow to reattach. The flow at $M = 0.28$ is entirely subsonic, because the critical $C_p (= -8.06)$ is not reached. Figure 8b presents baseline and controlled pressure distributions at $M = 0.4$ and $\alpha = 11$ deg. The baseline flow separates at $X/c \approx 0.2$. When excitation is applied, a pressure distribution similar to the one measured at $M = 0.28$, with control, is obtained. The only significant difference is that the upper surface flow, close to the LE, becomes supersonic as the excitation is activated ($C_{p,\mathrm{crit}} = -3.66$). Because the flow turns subsonic again upstream of the excitation slot, one should not expect significant compressibility effects on the controlled flow.

Figure 9a presents the steady and fluctuating wake-pressure distributions measured at $M = 0.28$, $\alpha = 14$ deg, and $R_c = 12.7 \times 10^6$, with and without excitation. The baseline wake could not be scanned in its entirety because of mechanical limitation on the travel of the wake rake. Therefore it had to be extrapolated in order to estimate the total drag. When a linear extrapolation was used to evaluate the baseline drag, the total drag coefficient was about 0.18. When excitation was activated, the drag was reduced to 0.085. These values compare favorably with the measured reduction in form drag, from 0.18 to 0.09, as shown in Fig. 7 for $\langle c_\mu \rangle = 30 \times 10^{-5}$. The fluctuating part of the baseline wake is skewed and presents a much higher fluctuation level on the upper side, corresponding to the flow that separated from the upper surface of the airfoil. A significant reduction of the wake unsteadiness was obtained as a result of the excitation at $F^+ = 2$. An integration of the fluctuating wake momentum, in the form

$$\frac{1}{qc} \int_{-\infty}^{\infty} p' \, \mathrm{d}Y \tag{2}$$

indicates a reduction of 34% in the unsteadiness of the controlled flow (without extrapolating the fluctuating part of the baseline wake).

Figure 9b presents the baseline and controlled wake pressure spectra, measured at $M = 0.28$, $\alpha = 14$ deg, $X/c = 2.1$. These Y/c positions were selected because the pressure fluctuations reach a maximum, and $\mathrm{d}P/\mathrm{d}Y$ is high on the upper side of the wake. It also corresponds to the upper, controlled surface of the airfoil. The baseline spectra show several peaks between $F^+ = 0.4$ to 0.7. When excitation is applied, the level of pressure fluctuations in the wake decreases over the entire frequency range. The most significant reduction is in the frequency range $F^+ < 1$. The level of the pressure fluctuations at the excitation frequency, $F^+ \cong 2$, is not higher than the fluctuation of the uncontrolled wake. This indicates that the oscillatory momentum which was introduced through the excitation slot was used primarily to modify the mean flow and transformed to smaller scales that dissipate rapidly in the attached regions of the turbulent boundary layer.

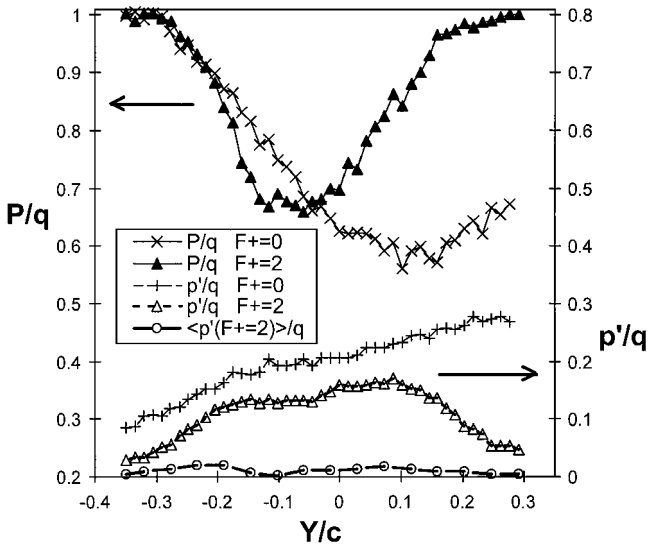

Fig. 9a NACA 0015 total, fluctuating and phase-locked wake pressures. $R_c = 12.7 \times 10^6$, $\alpha = 14$ deg, $M = 0.28$, $\langle c_\mu \rangle = 0.03\%$.

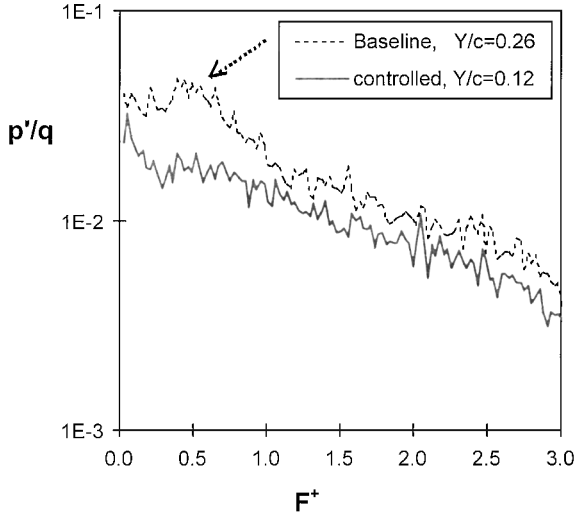

Fig. 9b Pressure spectra, conditions as in Fig. 9a.

The global effect of the excitation frequency, on the unsteadiness of the wake, can be evaluated by examining the amplitude distribution of the fundamental excitation frequency in the entire wake. Figure 9a also present the phase-locked pressure fluctuations measured in the wake $\langle p'(F^+ = 2) \rangle$ corresponding to the excitation frequency. It has the shape of the wake sinuous mode,[22] which can be interpreted as alternate sign vortex shedding every half-cycle from the upper and lower surfaces of the airfoil. The maximum level of the pressure fluctuations at the excitation frequency is very low, about 1%.

Data were also acquired at $M = 0.45$ and 0.5 at $R_c = 12.7 \times 10^6$ and 19×10^6. Significant R_c effects were identified in these mildly compressible flow conditions that make it difficult to identify changes in the effectiveness of the excitation. Another difficulty stems from the fact that the shock position varied but was always downstream of the fixed blowing slot (located at $X/c = 0.1$). Here we chose to present the results for $M = 0.55$ at $R_c = 19 \times 10^6$ that contain strong compressibility effects and a shock position closer to the slot, but still downstream of it.

Figure 10 presents compressible baseline and controlled lift data. It shows that the baseline $C_{l,\max}$ for $M = 0.55$ dropped to 1 at $\alpha_{\max} = 6$ deg from 1.31 at $\alpha_{\max} = 12$ deg for $M = 0.28$ (Fig. 6) and 1.17 at 9 deg for $M = 0.4$ (also in Fig. 6). Poststall lift decreases relative to $C_{l,\max}$. Unlike in the wholly incompressible flow, where surface tangential oscillatory excitation did not have any detrimental

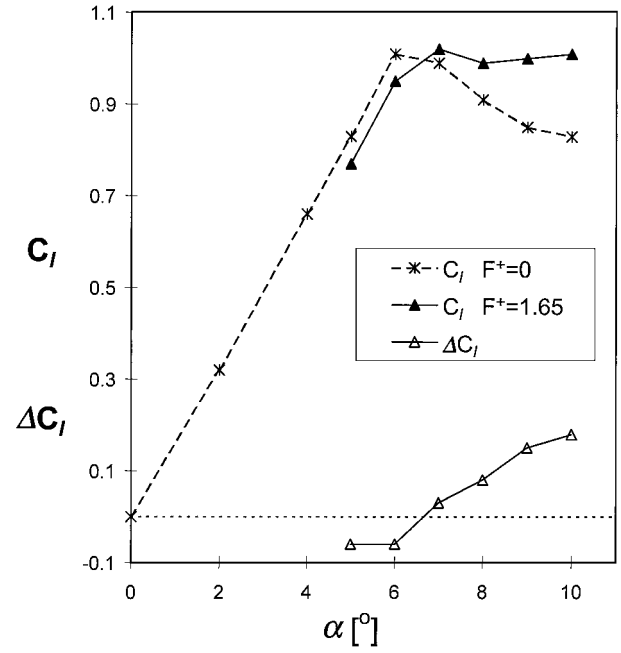

Fig. 10 Effects of periodic excitation on lift of the NACA 0015 airfoil. $R_c = 19 \times 10^6$, $M = 0.55$, $\langle c_\mu \rangle = 0.015\%$.

effect, a small decrease in lift as a result of activating the excitation can be observed at prestall angles of attack, at $M = 0.55$ (note ΔC_l that is also plotted in Fig. 10). An examination of the airfoil pressure distributions reveals that the reason for this performance degradation is a localized disturbance that was created at the excitation slot, upstream of the naturally occurring shock wave. One possible interpretation is that the disturbance thickens the very thin boundary layer, which in turn weakens the shock or increases its unsteadiness and eventually leads to earlier TE separation (Fig. 11b). At post stall α the excitation maintains C_l at about one while the baseline lift drops gradually to 0.85 (Fig. 10). As mentioned before, high lift is seldom required at transonic speeds, because the sizing of the wing is made to meet takeoff requirements. The important aspects of active separation control at compressible speeds are to delay the occurrence of drag divergence as a result of flow separation, to delay the onset and to alleviate the effects of buffet.

Figure 11a presents the baseline and controlled airfoil surface-pressure distributions at poststall angle of attack ($\alpha = 9$ deg). The baseline C_p shows a supersonic flow region near the LE that turns subsonic via a strong and possibly unsteady shock wave. The unsteadiness of the shock strength and position can be evaluated from observing the smeared foot of the shock. The mean position of the shock foot is at $X/c = 0.15$. The separated flow is manifested as a mild pressure recovery downstream of the baseline shock position and negative $C_{p,\mathrm{TE}}$. The presence of a mild pressure recovery over the separated region could be attributed to shock-wave enhanced turbulence.[17] This also is different from low-Mach-number separated flow, where very little or no pressure recovery is seen downstream of separation. As excitation was applied from the $X/c = 0.1$ slot (i.e., upstream of the averaged shock position and inside the supersonic flow), a number of changes could be observed. The flow upstream of the shock accelerates. This could be a result of two possible mechanisms.[22] The excitation and the resulting enhanced mixing thins the relatively thick boundary layer upstream of the shock. In turn the boundary layer accelerates, and a stronger shock is required to turn the flow subsonic again. The stronger shock also causes immediate flow separation downstream of it. The other mechanism is enhanced mixing downstream of the shock. This allows the turbulent boundary layer to close the separation bubble faster, resulting in a stronger pressure recovery and an enhanced capability to handle the stronger shock without catastrophic separation. It is assumed that both mechanisms are presently active. Indeed, the controlled shock is stronger, and its foot is less smeared than in the

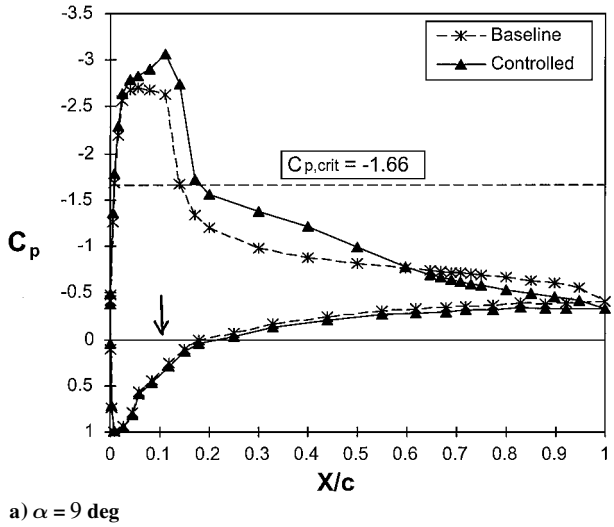

a) $\alpha = 9$ deg

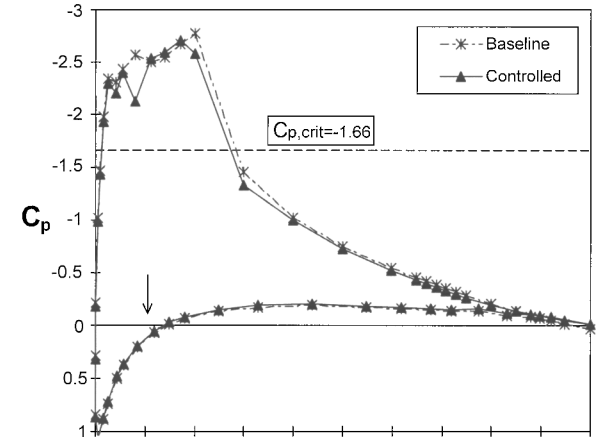

b) $\alpha = 6$ deg

Fig. 11 Baseline and controlled airfoil pressures. $R_c = 19 \times 10^6$, $M = 0.55$, $F^+ = 1.65$, $\langle c_\mu \rangle = 0.015\%$. → indicates excitation slot.

baseline flow. The pressure distribution downstream of the shock indicates that a large unsteady separation bubble exists between $0.2 < X/c < 0.6$. A more favorable pressure recovery can be seen at $X/c > 0.6$, and $C_{p,\mathrm{TE}}$ becomes more positive. Clearly, the controlled flow at compressible speeds is significantly more complex than its incompressible counterpart.

The averaged and fluctuating wake pressures for $M = 0.55$ and $\alpha = 9$ deg are presented in Fig. 12. Here also, the mechanical limitations on the movement of the wake rake prevented measurement of the entire baseline wake. The width of the wake decreased significantly, while the maximum wake deficit increased somewhat, with active excitation. This could be a result of a more stationary wake. The wake fluctuating pressure also restored a more symmetrical, double peak structure, because of the excitation. A major reduction in the wake unsteadiness can be observed on the upper side of the wake (i.e., $Y/c > 0$).

Figure 13a presents the drag, Fig. 13b presents the TE pressure, $C_{p,\mathrm{TE}}$, and Fig. 13c presents the integrated wake unsteadiness as defined in Eq. (2) for the compressible baseline and controlled data. The severe drag divergence starts at $\alpha > 4$ deg, as supersonic flow turns subsonic through a strong shock wave. The drag increases five fold (Fig. 13a), and the integrated wake unsteadiness increases six fold (Fig. 13c) between $\alpha = 4$ and 8 deg. $C_{p,\mathrm{TE}}$ becomes negative only between $\alpha = 6$ and 7 deg, indicating the development of TE separation. The majority of the drag divergence, certainly up to 6 deg, was caused by wave drag and was not caused by TE flow separation. It should not be expected that separation control would reduce drag where the flow is fully attached.

For $\alpha \leq 8$ deg the excitation results in a minor increase in drag (Fig. 13a), as well as in the wake unsteadiness (Fig. 13c), and a

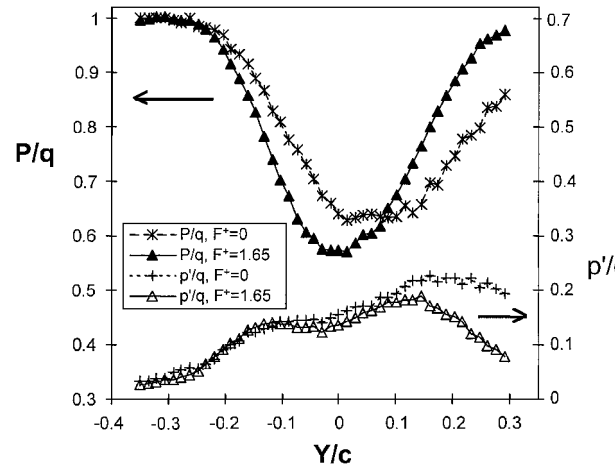

Fig. 12 Baseline and controlled wake pressures. $R_c = 19 \times 10^6$, $M = 0.55$, $\alpha = 9$ deg, $F^+ = 1.65$, $\langle c_\mu \rangle = 0.015\%$.

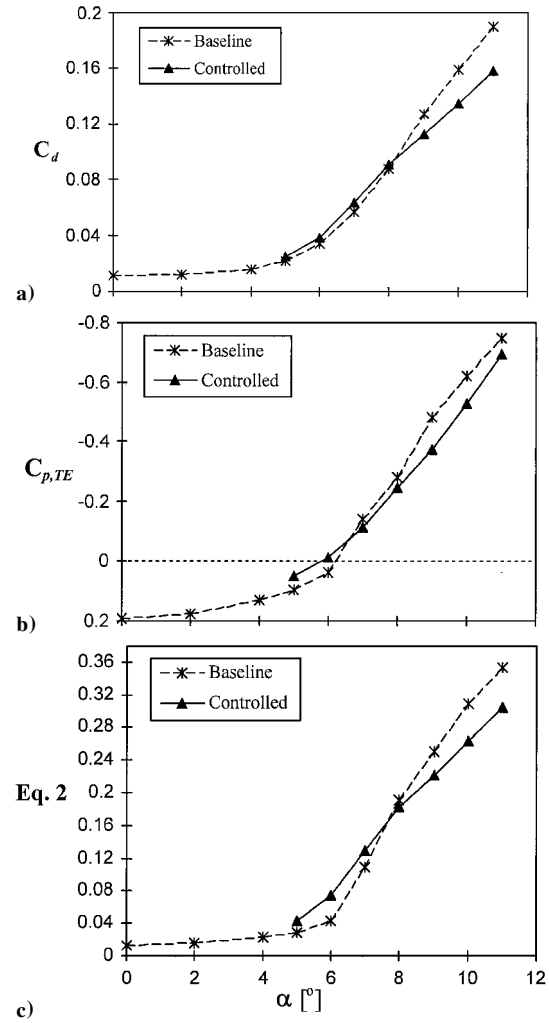

Fig. 13 Baseline and controlled airfoil drag, (a) TE pressure, (b) wake unsteadiness, and (c) $R_c = 19 \times 10^6$, $M = 0.55$, $F^+ = 1.65$, $\langle c_\mu \rangle = 0.015\%$.

small but detrimental effect on $C_{p,\mathrm{TE}}$ (Fig. 13b). These effects accompany the prestall reduction in the controlled lift, observed in Fig. 10. It remains to be seen if these effects will disappear once excitation is introduced closer to or downstream of the shock wave. For $\alpha > 8$ deg the excitation reduces the drag by 11–17%. A similar decrease can be observed in the integrated wake unsteadiness and in the tendency of $C_{p,\mathrm{TE}}$ to increase as a result of the excitation. Again, these benefits were obtained when excitation was applied upstream

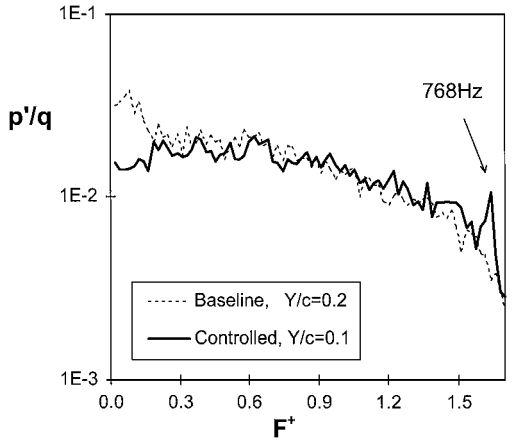

Fig. 14 Baseline and controlled wake spectra. $R_c = 19 \times 10^6$, $M = 0.55$, $\alpha = 9$ deg, $F^+ = 1.65$, $\langle c_\mu \rangle = 0.015\%$.

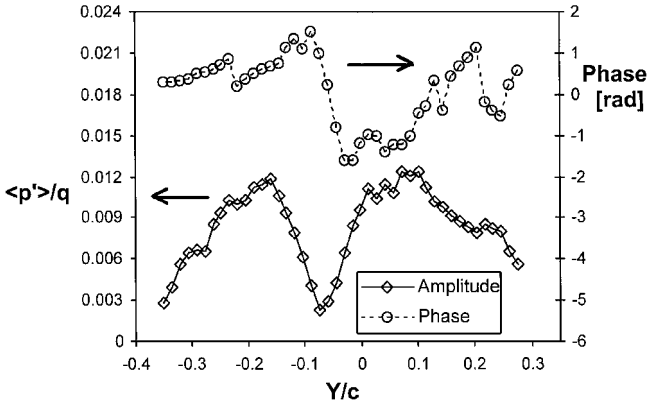

Fig. 15 Amplitude and phase distributions at the excitation frequency. Corresponding to the data of Fig. 16. $M = 0.55$.

of the mean shock position inside the supersonic flow. The efficiency of the excitation, in terms of $\langle c_\mu \rangle$, seems to be lower than in the incompressible flow conditions. It is not evident what effects the passage through and under the shock wave have on the vorticity of the excitation. Experimental[17] and numerical[18,20,21] evidence indicate that the excitation might even be amplified.

The spectra of the baseline and the controlled wake pressure fluctuations at $\alpha = 9$ deg are presented in Fig. 14. The Y/c locations presented were selected because they correspond to $C'_{p\,\max}$. It demonstrates that the baseline wake at $M = 0.55$ does not contain a distinctive shedding frequency, rather it has a wide band of high-amplitude fluctuations at $F^+ < 0.2$. These are typical buffeting frequencies. The controlled wake shows a significant reduction in the level of wake-pressure fluctuations, in the low-frequency range ($F^+ < 0.2$). When the level of the pressure fluctuations between 1 and 800 Hz (that includes the forcing frequency) is calculated, a reduction of about 11% is obtained (see also Fig. 12). The controlled data show a distinct peak only at the excitation frequency ($F^+ = 1.65$).

The wake-pressure fluctuations, phase locked to the excitation frequency, and the corresponding phase distribution of the fundamental excitation frequency ($F^+ = 1.65$) were calculated in order to check the effect of the wake motion that is related to the excitation and are plotted in Fig. 15. The amplitude and phase distributions are similar to the theoretically predicted distribution for a sinuous wake mode.[23] The phase is less coherent on the upper edge of the wake, corresponding to the controlled flow, but the shape is close to the theoretical prediction and to experiments. The maximum amplitude of the phase-locked wake-pressure fluctuations is about 1%, as in the incompressible data (Fig. 9a).

Figure 16 presents the improvement in the airfoil integral parameters as the excitation magnitude $\langle c_\mu \rangle$ is increased at $M = 0.55$ and

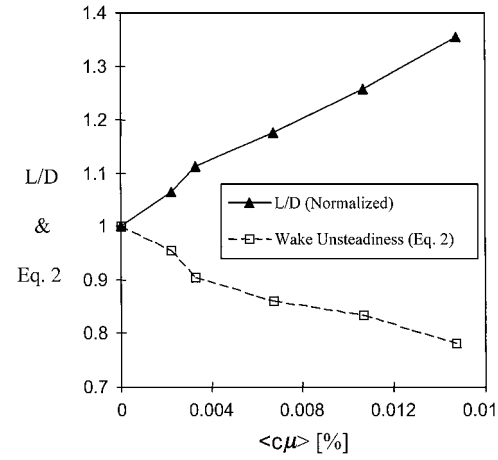

Fig. 16 Baseline and controlled airfoil lift-to-drag ratio and integrated wake unsteadiness vs excitation magnitude, both normalized by their baseline values. $R_c = 19 \times 10^6$, $M = 0.55$, $F^+ = 1.65$, $\alpha = 9$ deg.

$\alpha = 9$ deg. The data show that the relative lift-to-drag ratio increases by 35% in an almost linear manner with the increase in $\langle c_\mu \rangle$. This trend is highly desirable for the construction of a linear controller. The wake gradually becomes steadier as the lift-to-drag ratio increases as a result of increased excitation magnitude (Fig. 16). The averaged pressure gradient downstream of the active excitation slot increased by 50%, and $C_{p,\mathrm{TE}}$ increased by 30% as a result of the excitation with $F^+ = 1.65$ and $\langle c_\mu \rangle = 0.015\%$ (not shown). This indicates that the preceding benefits were obtained as a result of an increased tendency for flow reattachment.

IV. Conclusions

Active separation control was applied from the LE region of a straight NACA 0015 airfoil, initially in incompressible flow. Then the Mach number was gradually increased to cover compressible flows at flight Reynolds numbers. Strong Reynolds-number effects were identified in the airfoil baseline performance at moderately compressible flow conditions and poststall angles of attack. It makes the identification of clear trends in the controlled data difficult. The R_c effects weaken as the Mach number increases and a stronger shock develops.

It was demonstrated, in accordance with low-Reynolds-number experiments, that incompressible $C_{l,\max}$ can be increased by 15%, poststall lift can be increased by as much as 50%, and poststall drag can be reduced by more than 50% using low-momentum oscillatory excitation applied close to the leading edge. The controlled wake is also steadier. An important application is simplifying high-lift systems, reducing the weight, cost, and maintnance.

The significant increase in lift and lift-to-drag ratio, obtainable in incompressible speeds, should not be expected at compressible speeds. The global effect of the method is to accelerate the upstream boundary layer caused by the delay of boundary-layer separation. In compressible speeds this could lead to a stronger shock wave that in turn causes a more severe separation, which is less responsive to control. This process saturates the effectiveness of the excitation. Also, at increased Mach number the required frequencies increase at least linearly with the flow speed while the available $\langle c_\mu \rangle$ is inversely proportional to the dynamic pressure. In transonic flow the method could be used to alleviate buffet and control local separations rather than generating higher lift.

When excitation was applied well upstream of the shock wave, it had a detrimental effect on lift, drag, and wake steadiness. This is because of the creation of a localized disturbance at the blowing slot. This effect is not present in low Mach numbers. There, the introduction of wall-tangential excitation, far upstream of the boundary-layer separation, resulted in a smaller performance increment (when compared to excitation that was introduced immediately upstream of the separation), but did not result in absolute performance degradation.

It seems that the ability of similar $\langle c_\mu \rangle$ levels to reduce drag and wake unsteadiness decreases as the Mach number increases. But because of the great sensitivity of the relative location between the blowing slot and the mean shock position, it remains to be seen how the efficiency will vary once this parameter is better controlled.

The excitation became effective when it was introduced only slightly upstream of the shock wave, increasing the lift-to-drag ratio, reducing the drag, and causing a steadier wake. Very low levels of phase-locked wake-pressure fluctuations, at the excitation frequency, were measured in the controlled wake. A strong sensitivity of C_l, C_d, and wake unsteadiness on $\langle c_\mu \rangle$ was identified. The sensitivity to F^+ is weaker, in accordance with low-speed experiments.

Based on numerous experiments, it could safely be stated that whenever controlled excitation was applied close enough to the separation location it proved beneficial, regardless of the Mach number.

Acknowledgment

This work was performed while the first author held a National Research Council–NASA LaRC research associateship. The authors would like to thank W. L. Sellers III, M. Walsh, R. Joslin, C. B. McGinley, J. F. Barthelemy, and R. W. Wlezien for their continued support. The authors would also like to thank B. K. Stewart and the entire 0.3-m TCT crew from Langley Research Center for their support.

References

[1]Delery, J. M., "Shock Wave/Turbulent Boundary Layer Interaction and Its Control," *Progress in Aerospace Sciences*, Vol. 22, No. 4, 1985, pp. 209–280.

[2]McCormick, D. C., "Shock-Boundary Layer Interaction with Low Profile Vortex Generators and Passive Cavity," *AIAA Journal*, Vol. 31, No. 1, 1993, p. 96.

[3]Wallis, R. A., and Stuart, C. M., "On the Control of Shock-Induced Boundary-Layer Separation with Discrete Air Jets," Aeronautical Research Council C.P. No. 595, Jan. 1962.

[4]Mounts, J. S., and Barber, T. J., "Numerical Analysis of Shock-Induced Separation Alleviation Using Vortex Generators," AIAA Paper 92-0751, Jan. 1992.

[5]Krogmann, P., and Stanewsky, E., "Effects of Suction on Shock/Boundary-Layer Interaction and Shock Induced Separation," *Journal of Aircraft*, Vol. 22, Jan. 1985, pp. 37–42.

[6]Scott, M. A., Montgomery, R. C., and Weston, R. P., "Subsonic Maneuvering Effectiveness of High Performance Aircraft Which Employ Quasi-Static Shape Changes Devices," 36th Society of Photo-Optical Instrumentation Engineers, March 1998.

[7]Gad-el-Hak, M., and Bushnell, D. M., "Separation Control: Review," *Journal of Fluids Engineering*, Vol. 113, March 1991, pp. 5–30.

[8]Seifert, A., Bachar, T., Koss, D., Shepshelovich, M., and Wygnanski, I., "Oscillatory Blowing, a Tool to Delay Boundary Layer Separation," *AIAA Journal*, Vol. 31, No. 11, 1993, pp. 2052–2060.

[9]Seifert, A., Darabi, A., and Wygnanski, I., "On the Delay of Airfoil Stall by Periodic Excitation," *Journal of Aircraft*, Vol. 33, No. 4, 1996, pp. 691–699.

[10]Seifert, A., and Pack, L. G., "Oscillatory Control of Separation at High Reynolds Numbers," *AIAA Journal*, Vol. 37, No. 9, 1999, pp. 1063–1071.

[11]Wu, J. Z., Lu, X. Y., Denny, A. G., Fan, M., and Wu, J. M., "Post-Stall Flow Control on an Airfoil by Local Unsteady Forcing," *Journal of Fluid Mechanics*, Vol. 371, Sept. 1998, pp. 21–58.

[12]Donovon, J. F., Kral, L. D., and Cary, A. W., "Active Flow Control Applied to an Airfoil," AIAA Paper 98-0210, Jan. 1998.

[13]Szumowski, A. P., and Meier, G. E. A., "Forced Oscillations of Airfoil Flows," *Experiment in Fluids*, Vol. 21, 1996, pp. 457–464.

[14]Seifert, A., and Pack, L. G., "Oscillatory Excitation of Unsteady Compressible Flows over Airfoils at Flight Reynolds Numbers," AIAA Paper 99-0925, Jan. 1999.

[15]Rallo, R. A., Dress, D. A., and Siegle, H. J. A., "Operating Envelope Charts for the Langley 0.3-Meter Transonic Cryogenic Wind Tunnel," NASA TM-89008, Aug. 1986.

[16]Ladson, C. A., and Ray, E. J., "Evolution, Calibration, and Operational Characteristics of the Two-Dimensional Test Section of the Langley 0.3-Meter Transonic Cryogenic Tunnel," NASA TP-2749, Sept. 1987.

[17]Delery, J. M., "Investigation of a Strong Shock Turbulent Boundary Layer Interaction in a 2-D Transonic Flows with Emphasis on Turbulence Phenomena," AIAA Paper 81-1245, June 1981.

[18]Nixon, D., Keefe, L. R., and Rodman, L. C., "Turbulence Amplification Through a Shock-Wave," AIAA Paper 92-0313, Jan. 1992.

[19]Ribner, H. S., "Convection of a Pattern of Vorticity Through a Shock-Wave," NACA 1164, Jan. 1954.

[20]Kao, C. T., von Ellenrieder, K., MacCormack, R. W., and Bershader, D., "Physical Analysis of Two-Dimensional Compressible Vortex-Shock Interaction," AIAA Paper 96-0044, Jan. 1996.

[21]Guichard, L., Vervisch, L., and Domingo, P., "Numerical Study of the Interaction Between a Mixing Zone and a Pressure Discontinuity," AIAA Paper 95-0877, Jan. 1995.

[22]Chang, P. K., *Separation of Flow*, Perganon, New York, 1970, pp. 227–228.

[23]Marasly, B., Champagne, F. H., and Wygnanski, I., "Effects of Travelling Wave on the Growth of a Turbulent Wake," *Journal of Fluid Mechanics*, Vol. 235, Feb. 1992, pp. 511–528.